

The Infinite Chain Nitride Na₅Ba₃N. A One-Dimensional Void Metal?

G. Jeffrey Snyder[†] and Arndt Simon*

Contribution from the Max-Planck-Institut für Festkörperforschung, Heisenbergstrasse 1, 70569 Stuttgart, Germany

Received October 3, 1994[⊗]

Abstract: The crystal structure of Na₅Ba₃N was determined from a single crystal grown by a diffusion limited process (*Pnma*, $a = 11.882(2) \text{ \AA}$, $b = 7.049(1) \text{ \AA}$, $c = 17.792(4) \text{ \AA}$, $Z = 4$, $R = 0.063$). The structure contains Ba₃N chains nearly identical with those found in NaBa₃N. The structure can be explained in terms of strong Ba–N intrachain ionic bonding and weak Ba–Na metallic bonding separating the chains. Na₅Ba₃N is a common impurity phase in Na–Ba alloys, which has probably exacerbated the difficulties in determining Na–Ba phase equilibria. Na₅Ba₃N has the structural characteristics of a one-dimensional void metal.

Introduction

In the last decade there has been a surge of interest in nanometer scale structures and the mesoscopic physics involved. One example is the quantum dot (anti quantum dot) array: a two-dimensional electron gas in which a periodic array of conducting (insulating) dots has been patterned. In this case the physics involved are semiclassical. In order to achieve quantum size effects, much smaller structures are needed.¹ On the atomic scale, one-dimensional metallic systems are realized in a number of compounds which contain metallic chains in a nonmetallic matrix. Krogmann's columnar structures² may serve as an example where electronic delocalization occurs in linear platinum atom chains, each of which represents a "nanowire".

In analogy to anti-quantum-dot arrays, one can imagine a system of anti-nanowires, requiring chains of anions repulsive to conduction electrons embedded in a metallic matrix. Such void metals where conduction electrons are excluded from regions within the structure are rare. The best-known such materials are the suboxides of rubidium and cesium³ which form an array of (zero dimensional) clusters that repel conduction electrons. One consequence of quantum size effects is the work function of these materials being greatly reduced due to quantum confinement of the conduction electrons.⁴ These compounds have found practical application as the active surface in infrared photocathodes.⁵

The recent discovery⁶ of NaBa₃N has opened the unusual chemistry of the alkali metal suboxides to the alkaline earth nitrides. The new compound Na₅Ba₃N, containing much more sodium, clearly has the structural attributes of a one-dimensional void metal.

Experimental Section

Sample Preparation. Sodium rich liquid alloys of sodium–barium readily absorb nitrogen gas. Upon cooling, the most common nitrogen-

[†] Present address: Department of Applied Physics, Stanford University, Stanford, CA 94305.

[⊗] Abstract published in *Advance ACS Abstracts*, February 1, 1995.

(1) Weiss, D.; Roukes, M. L.; Menshig, A.; Grambow, P.; von Klitzing, K.; Weimann, G. *Phys. Rev. Lett.* **1991**, *66*, 2790.

(2) Krogmann, K. *Angew. Chem.* **1969**, *81*, 10; *Angew. Chem., Int. Ed. Engl.* **1969**, *8*, 35.

(3) Simon, A. *Structure Bond.* **1979**, *36*, 81.

(4) Burt, M. G.; Heine, V. *J. Phys. C* **1978**, *11*, 961.

(5) Ebbinghaus, G.; Braun, W.; Simon, A.; Berresheim, K. *Phys. Rev. Lett.* **1976**, *37*, 1770.

(6) Rauch, P. E.; Simon, A. *Angew. Chem.* **1992**, *104*, 1505; *Angew. Chem., Int. Ed. Engl.* **1992**, *31*, 1519.

containing precipitate is Na₅Ba₃N, the stoichiometry of which was determined by the structural study in this work. For example, a 1 g mixture of Na:Ba:N with an atomic ratio of 46:6:1 was brought into a 0.2 mm diameter X-ray capillary. The X-ray diffraction of this polycrystalline material showed Na, Na₂Ba, and Na₅Ba₃N. In all diffraction patterns taken while the temperature was continuously increased, Na₅Ba₃N disappears at approximately 67 °C, which is close to the eutectic temperature in the Ba–Na system.

Attempts to grow X-ray diffraction size single crystals for structure solution in these samples have failed. Voids in the sodium–barium flux often contained long crystals of Na₅Ba₃N on the inside walls of the glass capillary, with their *b*-axis along the capillary axis. However, these crystals were far too small for structure determination.

In order to grow suitable crystals for structure solution, a diffusion-limited process was utilized. A capillary size sample of composition Na_{0.8}Ba_{0.2}, as described in ref 7, was ultimately sealed under nitrogen gas as opposed to argon. The entire sample was slowly heated (2°/h) to 200 °C and then cooled from the melt at 1°/h in an aluminum core furnace. There was no apparent reaction of the sample with the glass at these temperatures. Crystals of NaBa₃N have also been grown in a similar manner.

X-ray Crystallography. A suitable crystal was found near the tip of the sample and centered using axial photographs of a CAD-4 diffractometer, which was also used for data collection. Other smaller crystals of Na₅Ba₃N as well as sodium metal were also in the X-ray beam as evident from the axial photographs. Twenty four reflections in the 19–24° θ range were used for cell determination. Within experimental error these cell parameters are the same as those observed in powder diffraction measurements.

Results

Structure Solution. The crystal structure of Na₅Ba₃N was solved using direct methods and refined using SHELX-93 and related software. Data with *d*-spacing less than 0.83 Å were omitted for the refinement but included in the calculations for the all data *R* value. Absorption was calculated empirically using ψ -scans. Details of the single crystal data collection are summarized in Table 1 and the final atomic positional and anisotropic thermal displacement parameters are given in Tables 2 and 3.

Description of Structure. The barium and nitrogen atoms of Na₅Ba₃N are arranged in an infinite chain, Ba₃N, of face sharing barium octahedra centered by nitrogen atoms, almost exactly the same as found in NaBa₃N. The Ba₃N chains in Na₅Ba₃N form a slightly distorted hexagonal rod packing along *b*, similar to the perfect triangular lattice of Ba₃N chains in

(7) Snyder, G. J.; Simon, A. *Z. Naturforsch. B* **1994**, *49B*, 189.

Table 1. Crystal Data and Structure Refinement for $\text{Na}_5\text{Ba}_3\text{N}$

diffractometer type	CAD-4
monochromator	graphite
scan type	$\omega-2\theta$
formula wt	540.98
temp, K	293(2)
wavelength, Å	0.71073
crystal system	orthorhombic
space group	$Pnma$ (No. 62)
unit cell dimensions	
<i>a</i> , Å	11.897(3)
<i>b</i> , Å	7.056(2)
<i>c</i> , Å	17.801(3)
α , deg	90
β , deg	90
γ , deg	90
volume, Å ³	1494.3(6)
<i>Z</i>	4
density (calcd), g/cm ³	2.405
absorption coeff, mm ⁻¹	7.910
<i>F</i> (000)	920
θ range for data collection, deg	2.06–29.98
index ranges	$0 \leq h \leq 16, 0 \leq k \leq 9,$ $-25 \leq l \leq 24$
no. of reflns collected	4601
no. of independent reflns	2332 ($R_{\text{int}} = 0.1271$)
refinement method	full-matrix least-squares on F^2
no. of data/restraints/parameters	1490/0/52
goodness-of-fit on F^2	1.666
final <i>R</i> indices [$I > 2\sigma(I)$]	$R_1 = 0.0638, wR_2 = 0.1186$
<i>R</i> indices (all data)	$R_1 = 0.1132, wR_2 = 0.1344$
largest diff peak and hole, Å ⁻³	2.573 and -1.104

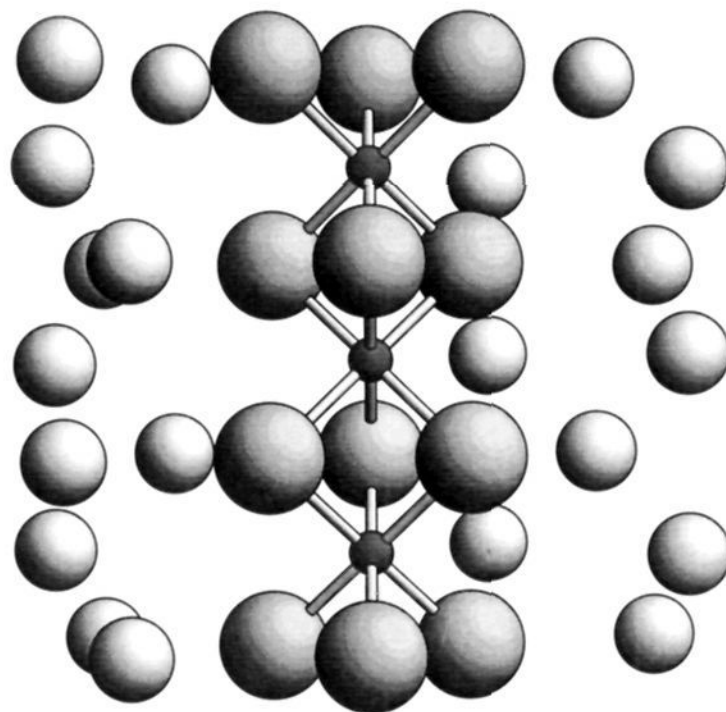
Table 2. Atomic Coordinates and Equivalent Isotropic Displacement Parameters [10^4Å^2] for $\text{Na}_5\text{Ba}_3\text{N}$, where $U(\text{eq})$ Is Defined As One-Third of the Trace of the Orthogonalized U_{ij} Tensor

atom	position	<i>x</i>	<i>y</i>	<i>z</i>	<i>U</i> (eq)
Ba(1)	4c	0.11628(9)	1/4	0.58746(7)	325(3)
Ba(2)	4c	0.05490(10)	1/4	0.38765(6)	334(3)
Ba(3)	4c	0.32833(9)	1/4	0.97556(7)	319(3)
Na(1)	4c	0.1692(8)	1/4	0.1678(6)	680(3)
Na(2)	4c	0.3742(8)	1/4	0.7385(6)	630(3)
Na(3)	4c	0.4450(9)	1/4	0.5097(7)	780(3)
Na(4)	8d	0.1220(6)	0.9900(11)	0.8149(5)	830(2)
N	4b	0	0	1/2	320(3)

Table 3. Anisotropic Displacement Parameters [10^4Å^2] for $\text{Na}_5\text{Ba}_3\text{N}$, Where the Anisotropic Displacement Factor Exponent Takes the Form $-2\pi^2[(ha^*)^2U_{11} + \dots + 2hka^*b^*U_{12}]$

	U_{11}	U_{22}	U_{33}	U_{23}	U_{13}	U_{12}
Ba(1)	380(6)	227(5)	369(6)	0	-82(5)	0
Ba(2)	485(6)	227(5)	289(6)	0	83(6)	0
Ba(3)	334(5)	226(5)	399(7)	0	-31(5)	0
Na(1)	750(6)	700(7)	600(6)	0	140(5)	0
Na(2)	750(6)	500(5)	660(7)	0	-220(5)	0
Na(3)	650(6)	940(8)	740(7)	0	20(6)	0
Na(4)	780(4)	590(4)	1130(6)	-10(5)	-230(5)	0(4)
N	440(7)	210(7)	300(7)	0(7)	100(7)	30(6)

NaBa_3N . The Ba–N distance in $\text{Na}_5\text{Ba}_3\text{N}$ ranges from 2.729 to 2.743 Å, with an average value very close to the 2.734 Å Ba–N distance in NaBa_3N . These distances are actually shorter than the sum of the ionic radii (2.9 Å).⁸ Also like NaBa_3N which has two intrachain Ba–Ba distances of 3.645 and 4.076 Å, $\text{Na}_5\text{Ba}_3\text{N}$ has corresponding ranges of 3.601–3.632 Å and 4.092–4.102 Å, respectively, where the first is due to contacts in the plane perpendicular to the chain axis. Since the Ba–Ba in-plane distances, which are (statistically) significantly different, vary by only 0.4%, the 3-fold symmetry of the Ba_3N chains in

**Figure 1.** Ba_3N chain in $\text{Na}_5\text{Ba}_3\text{N}$. The large and medium size spheres represent barium and sodium atoms, respectively. The small darker spheres represent nitrogen atoms. Bonds are drawn between neighboring barium and nitrogen atoms.

NaBa_3N is approximately maintained. This is remarkable considering the different coordination to sodium atoms for each barium atom, indicating the rigidity of the Ba_3N chains due to strong Ba–N ionic bonding as opposed to weaker Ba–Na metallic bonding. Ba(1), Ba(2), and Ba(3) have 5, 7, and 4 sodium near neighbors, respectively, as compared to 4 for the barium atom in NaBa_3N . A side projection of a Ba_3N chain in $\text{Na}_5\text{Ba}_3\text{N}$ with its coordinating sodium atoms is shown in Figure 1.

The significant difference between $\text{Na}_5\text{Ba}_3\text{N}$ and NaBa_3N is the sodium atom content and arrangement. NaBa_3N has but one independent sodium atom coordinated to 12 barium atoms, and barely separates the Ba_3N chains. $\text{Na}_5\text{Ba}_3\text{N}$ has four very differently coordinated sodium atoms. The center-to-center distance between the Ba_3N chains is 10.70 Å as compared to 8.44 Å in NaBa_3N (Figures 2 and 3). Na(1) and Na(3) atoms both only coordinate to two barium atoms while Na(1) has seven Na near neighbors and the Na(3) atoms have eight. Na(2) and Na(4) atoms are both coordinated to twelve atoms, five of which are barium atoms for Na(2), while Na(4) has only four barium near neighbors.

The Ba–Na and Na–Na average distances of 4.3(2) and 3.9(2) Å, respectively, in $\text{Na}_5\text{Ba}_3\text{N}$ are similar to those found in the Na–Ba intermetallics NaBa (4.27, 3.72 Å)⁹ and Na_2Ba (4.32, 3.70 Å) and close to the sum of (12 coordinate) metallic radii (4.15, 3.82 Å). A complete list of atomic distances is given in Table 4.

Discussion

There are two separate aspects resulting from the discovery of $\text{Na}_5\text{Ba}_3\text{N}$. First our results on Na–Ba subnitrides, and $\text{Na}_5\text{Ba}_3\text{N}$ in particular, are relevant to previous work on Na–Ba alloy systems. We have frequently observed $\text{Na}_5\text{Ba}_3\text{N}$ via powder X-ray diffraction in many of our Na–Ba and Na–Ba–N samples. Trace amounts of nitrogen in sodium rich Na–Ba alloys usually form $\text{Na}_5\text{Ba}_3\text{N}$, which has two characteristic strong reflections, 101 and 002, at high *d*-spacing. The intensities of these reflections are further enhanced by orientation effects of these highly anisotropic crystals. Certain results on binary Na–Ba phases need to be revised. The most recent and

(8) Baur, W. H. *Cryst. Rev.* **1987**, *1*, 59.(9) Snyder, G. J.; Simon, A. *J. Chem. Soc., Dalton Trans.* **1994**, 1159.

interaction with silica which will act as “chemical glue”, followed by impregnation of a nickel salt, forming a “nickel reservoir” in weak interaction with the support.

In a previous work,³⁴ we have reported on the evidence of a growth mechanism of nickel particles onto the “chemical glue”, i.e. on “nickel nuclei”, after impregnation. Indeed, after thermal reduction under hydrogen, it has been possible to obtain nickel metal particles with average diameters between 20 and 60 Å, depending on the relative amounts of “nickel nuclei” and “nickel reservoir”.

However, several questions remained unanswered: (i) At which step of preparation or reduction does the nickel particle growth occur, and what kind of nickel leads to the formation of particles, nickel in the metallic or oxidized state? (ii) What is the mechanism of growth of the nickel particles?

The goal of the present work is an attempt to answer these questions and to document the approach given in the previous paper³⁴ by new results.

Experimental Section

(1) Sample Preparation. (a) Sample Preparation by a Two-Step Procedure. Step 1: Preparation of “Nickel Nuclei”. (1) By cation-exchange with hexaamminenickel(II), $[\text{Ni}(\text{NH}_3)_6]^{2+}$. The samples were prepared from a solution of ammonium nitrate (1 mol/L) to which nickel nitrate was added in order to obtain solutions with different concentrations (0.05, 0.025, and 0.001 mol/L). The solution pH was adjusted to 9.8 by bubbling gaseous NH_3 . At this pH, the main nickel species is $[\text{Ni}(\text{NH}_3)_6]^{2+}$.³⁵ This solution (70 cm³) was added to 5 g of silica. The suspensions were continuously stirred at 25 °C in a thermostated vessel for 24 h. Then, they were filtered and the samples were washed with a solution of ammonium nitrate (1 mol/L) at pH 9.8. The samples were dried for 24 h at 90 °C and then calcined in air at 500 °C for 2 h in order to decompose nitrate and hexaamminenickel(II). The samples are hereafter referred to as $\text{ENi}_{\text{NH}_3/x}/500$, where x is the nickel loading expressed in wt % of nickel per gram of dehydrated silica and 500 indicates the calcination temperature.

(2) By cation-exchange with tris(ethylenediamine)nickel(II), $[\text{Ni}(\text{en})_3]^{2+}$. The samples were prepared from solutions of $[\text{Ni}(\text{en})_3](\text{NO}_3)_2$ (0.5, 0.13, and 0.05 mol/L). These solutions were obtained with a mixture of nickel nitrate solutions and ethylenediamine. The concentration ratio $[\text{en}]/[\text{Ni}^{II}]$ was higher than 3 in order to form the $[\text{Ni}(\text{en})_3]^{2+}$ complex (pH \approx 12). The solution (80 cm³) was added to 5 g of silica. The suspensions were continuously stirred at 25 °C in a thermostated vessel for 48 h. Then, they were filtered and the samples were washed with a 0.24 M ethylenediamine solution at pH 12. The samples were dried at 90 °C for 24 h and then calcined in air at 600 °C for 2 h in order to decompose nitrate and (ethylenediamine)nickel(II). The samples $[\text{Ni}(\text{en})_3]^{2+}/\text{SiO}_2$ are hereafter referred to as $\text{ENi}_{\text{en}/x}/600$, where x is the nickel loading, and 600, the calcination temperature.

(3) By water-washing of impregnated Ni/SiO₂ samples. The impregnation of silica with nickel was performed by incipient wetness impregnation (2 mL/g) with an aqueous solution of nickel nitrate (3.4 mol/L; beyond this concentration, the solution is saturated). The mixture was kept at room temperature for 2 h before drying at 90 °C for 18 h. The nickel loading is 47 wt %. The sample was then thoroughly washed with water at room temperature through a Büchner until the water remained colorless. After water-washing, the Ni loading is less than 1% of the initial one. The amount of nonsoluble Ni was increased by performing several cycles of impregnation (47 wt % of Ni)—drying (90 °C/18 h)—water-washing—drying (90 °C/18 h). The water-washed impregnated samples are hereafter referred to as IWNi_x .

Step 2: Impregnation of the “Nickel Reservoir”. The “nickel reservoir” was obtained by impregnation of silica containing “nickel nuclei”, with different concentrations of nickel nitrate according to the method described above. The impregnating volume was 1.5 mL/g for the water-washed samples and 1 mL/g for the exchanged samples.³⁶

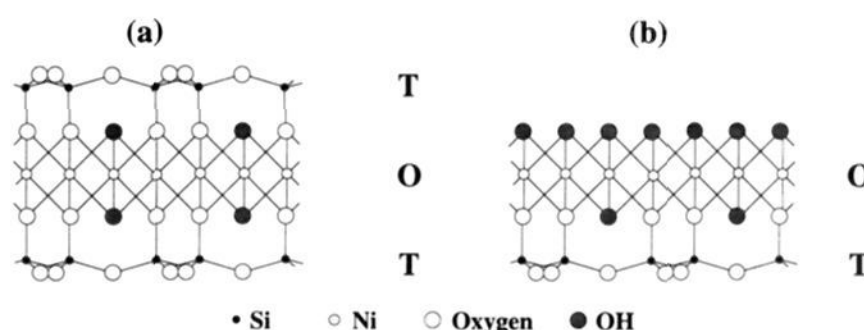


Figure 1. Projection on the bc plane of (a) a TOT layer of 2:1 nickel phyllosilicate and (b) a TO layer of 1:1 nickel phyllosilicate (ref 39).

These samples are referred to as $\text{IWNi}+\text{INi}$, $\text{ENi}_{\text{NH}_3}/500+\text{INi}$, and $\text{ENi}_{\text{en}}/600+\text{INi}$, depending on the nature of the nuclei.

(b) Reference Samples. The reference samples for the $\text{IWNi}+\text{INi}$ samples, referred to as INi , were prepared by impregnation as described above. The reference samples of the $\text{ENi}_{\text{NH}_3}/500+\text{INi}$ and $\text{ENi}_{\text{en}}/600+\text{INi}$ samples whose “nickel nuclei” were prepared in basic medium and under magnetic stirring, and then calcined, were obtained by impregnation of silicas previously submitted to the same conditions of exchange except for the presence of nickel, and then calcined. They are called $\text{NH}_3\text{-SiO}_2/500+\text{INi}$ and $\text{en-SiO}_2/600+\text{INi}$.

All the samples were prepared with silica Spherosil XOA400 (Rhône Poulenc, France, $S_{\text{BET}} = 400 \text{ m}^2/\text{g}$, pore volume = 1.25 cm³/g, average pore diameter = 80 Å).

(2) Techniques. Chemical analyses of nickel were performed in the Center of Chemical Analysis of the CNRS (Vernaison, France).

The XRD spectra were carried out on a Siemens diffractometer (D500). The phase identifications were performed by comparison with the tabulated JCPDS d-spacing files.

UV–visible–near-IR spectra were recorded on a Beckman 5270 reflectance spectrometer equipped with an integration sphere and a double monochromator. BaSO_4 was used as the reference.

EXAFS measurements at the absorption edge of Ni were performed at the LURE Radiation Synchrotron Facility (EXAFS I) using the X-ray beam emitted by the DCI storage ring (positron energy = 1.85 GeV, ring current = 300 mA). The spectra were recorded in transmission mode at room temperature using two air-filled ionization chambers. The energy was scanned with 2 eV steps from 8200 to 9200 eV (K absorption edge of Ni = 8331 eV), using a channel-cut single crystal of silicon as the monochromator. EXAFS measurements were carried out three times for each sample. The absorption variation through the edge $\Delta(\mu x)$ was at least 0.5.

The analyses of the EXAFS spectra were performed by following standard procedures for background removal, extraction of the EXAFS signal, and normalization to the edge absorption. Fourier transforms were obtained after multiplication of the EXAFS signal by a factor k^3 , using the same Hanning window for the references and the investigated systems. Data treatment was performed with the software “EXAFS pour le Mac”.³⁷

Amplitude and phase functions for O, Ni, and Si backscatters were experimentally obtained from the spectra of well-crystallized $\text{Ni}(\text{OH})_2$ and Ni-doped $\text{Mg}(\text{OH})_2$ ($\text{Ni}:\text{Mg}(\text{OH})_2$). The latter compound was considered as a reference for Si backscatters because the masses of Si and Mg are very close.³⁸ The distances, numbers of backscatters, and Debye–Waller factors ($\Delta\sigma^2$) are gathered in Table 1. Two synthetic nickel silicates with layer structures, a 2:1 phyllosilicate ($\text{Ni}_3\text{Si}_4\text{O}_{10}(\text{OH})_2$, also called talc) and a 1:1 phyllosilicate ($\text{Ni}_3\text{Si}_2\text{O}_5(\text{OH})_4$, also called nepouite)³⁹ (Figure 1), kindly supplied by A. Decarreau (Laboratoire de Pétrologie de la Surface, University of Poitiers, France), were used as references for the Debye–Waller factor calibration (Figure 2a,b, Table 1).

The samples were reduced by temperature-programmed reduction (TPR), from room temperature to 700 °C, with a heating rate of 7.5

(36) During the preparation by exchange, the use of both a basic solution which attacks silica and a magnetic stirrer caused the grinding of silica, and ground silica requires a lower impregnating volume to be wetted.

(37) (a) Michalowicz, A. Doctoral Thesis, Université Paris XII-Val de Marne, 1990. (b) Michalowicz, A. EXAFS Pour le Mac. In *Logiciels pour la Chimie*; Société Française de Chimie: Paris, 1991; p 102.

(38) Clause, O.; Kermarec, M.; Bonneviot, L.; Villain, F.; Che, M. *J. Am. Chem. Soc.* **1992**, *114*, 4709–4717.

(34) Cheng, Z. X.; Louis, C.; Che, M. *Z. Phys. D* **1991**, *20*, 445–448.

(35) Clause, O. Doctoral Thesis, Université Pierre et Marie Curie, Paris, 1989.

Table 5. Crystal Volumes for Na–Ba–N Compounds

compd	formula vol (Å ³)	vol contraction ^a (%)	residual vol ^b per BaN _n (Å ³)	ref
Na	39.5	0		
Ba	63.4	0	63.4	
Na ₂ Ba	142.0	0.33	63.0	7
NaBa	102.8	0.10	63.3	9
Na ₁₆ Ba ₆ N	982.8	2.95	58.5	13
Na ₅ Ba ₃ N	372.5	3.94	58.3	
NaBa ₃ N	215.4	6.27	58.6	6
Ba ₂ N	105.7	16.6	52.8	17
Ba ₃ N ₂	150.7	20.8	50.2	17

^a Volume contraction for Na_xBa_yN_z is $(xV_{\text{Na}} + yV_{\text{Ba}} - V_{\text{Na}_x\text{Ba}_y\text{N}_z}) / (xV_{\text{Na}} + yV_{\text{Ba}})$. ^b Residual volume for Na_xBa_yN_z is $(V_{\text{Na}_x\text{Ba}_y\text{N}_z} - xV_{\text{Na}}) / y$; $n = z/y$.

much as Ba itself forms intermetallics with Na. In contrast to NaBa₃N which has short interchain Ba–Ba contacts, Na₅Ba₃N has no such contacts, proving that such interactions are not necessary for Ba₃N chain formation. Again there is a close analogy with the alkali metal suboxides, where the ionic entities, e.g. Cs₁₁O₃ clusters, can be diluted by various amounts of excess alkali metal in stoichiometric compounds like Rb_xCs₁₁O₃, where $x = 0, 1, 2, 7$. In the same way, the Na atoms of Na_xBa₃N, $x = 1$ and 5 , separate the Ba₃N chains and are not involved in electron transfer to the nitrogen atoms. Indeed Cs_{3±3}O, also having a chain structure,¹⁵ would be the $x = 0$ analog of Na_xBa₃N.

The purely metallic nature of the Na atoms follows, not only from metal-like interatomic distances, but also from volume considerations. The intermetallic compounds Na₂Ba and NaBa contract only slightly upon phase formation as seen from the data in Table 5. Upon addition of nitrogen, a dramatic decrease in volume is observed. The Na atoms do not participate in this volume contraction, since they contribute a constant volume to all Na-containing compounds in Table 5, namely that of Na metal, 39.5 Å³. This is confirmed especially in the case of NaBa₃N and Na₅Ba₃N since the remaining volume of the Ba₃N units is identical for both compounds.¹⁶ The shrinkage of barium nitrides with respect to barium metal is due to the

(15) Tsai, K. R.; Harris, P. M.; Lassetre, E. N. *J. Phys. Chem.* **1956**, *60*, 345. Simon, A. Z. *Anorg. Allgem. Chem.* **1973**, *395*, 301.

(16) This consistency can help us determine the stoichiometry of yet unsolved crystal structures in the Ba–Na–N system. For example, we have found a compound that crystallizes in a hexagonal cell $a = 12.604$ Å, $c = 12.597$ Å which due to volume considerations could be either Na₁₂Ba₇N₃ or Na₉Ba₁₀N₆.

decrease in volume of the Ba atoms which even overcompensates for the additional volume of the N atoms. This shrinkage, in spite of the increased Coulombic repulsion, actually brings the barium atoms 0.5 Å closer in the nitrides than in the metal.

The preceding discussion raises the question as to the role of the Na in the compounds Na_xBa₃N. Since the compound without sodium, “Ba₃N”, does not exist, the sodium atoms seem to stabilize the Ba₃N chains. Normally, clusters are stabilized by ionic or covalent bonding of ligands. Here the stabilization is via metallic bonds. Since barium does not bond to potassium to form intermetallic compounds like it does with sodium, potassium is also unable to stabilize the formation of Ba₃N chains: there is no evidence of barium subnitrides with potassium. The sodium variability in the Ba₃N chains also opens possibilities of sodium variability in barium subnitrides with different barium-to-nitrogen ratios. For the hypothetical series Na_xBa₂N, where the sodium atoms would act as intercalation atoms between the Ba₂N layers, only the $x = 0$ binary¹⁷ is presently known.

Conclusion

A unique structural principle is realized with the compounds NaBa₃N and in particular Na₅Ba₃N. One can visualize these compounds as metals “drilled” with a periodic array of atomic scale bores, i.e. chains of N³⁻ ions which are expected to be repulsive to conduction electrons. So far, only the metallic nature of the compounds is known. Consequences of the peculiar void structure with respect to physical properties, e.g. work function, cyclotron resonance, etc., still have to be elucidated.

Acknowledgment. The authors thank Jean Rouxel and Paul Rauch for stimulating discussion, Horst Borrmann and Willi Röthenbach for their assistance in this project, and the Hertz Foundation for financial support.

Supplementary Material Available: Complete list of observed and calculated structure factors for Na₅Ba₃N (5 pages). This material is contained in many libraries on microfiche, immediately follows this article in the microfilm version of the journal, and can be ordered from the ACS, and can be downloaded from the Internet; see any current masthead page for ordering information and Internet access instructions.

JA943259O

(17) Künzel, H.-T. *Metallreiche Bariumnitride*, Thesis, University Stuttgart, 1980.